

## Article

# Comparison of Different Magnesium Hydroxide Coatings Applied on Concrete Substrates (Sewer Pipes) for Protection against Bio-Corrosion

Domna Merachtsaki <sup>1</sup>, Eirini-Chrysanthi Tsardaka <sup>2</sup>, Eleftherios K. Anastasiou <sup>2</sup>, Haris Yiannoulakis <sup>3</sup> and Anastasios Zouboulis <sup>1,\*</sup>

<sup>1</sup> Laboratory of Chemical and Environmental Technology, Department of Chemistry, Aristotle University of Thessaloniki, 54124 Thessaloniki, Greece; meradomn@chem.auth.gr

<sup>2</sup> Laboratory of Building Materials, Department of Civil Engineering, Aristotle University of Thessaloniki, 54124 Thessaloniki, Greece; extsardaka@gmail.com (E.-C.T.); elan@civil.auth.gr (E.K.A.)

<sup>3</sup> Research and Development Center, Grecian Magnesite S.A., 57006 Thessaloniki, Greece; h.yiannoulakis@grecianmagnesite.com

\* Correspondence: zoubouli@chem.auth.gr

**Abstract:** Several coatings and linings have been examined and used for the protection of sewer concrete pipes, against mainly biogenic-provoked corrosion due to the production of bio-sulfuric acid, leading to the degradation of the pipes' structure and eventually, to their collapse and need for costly replacement. This study aimed to examine the potential differences between five different magnesium hydroxide coatings, prepared from powders presenting different purity, surface area and pore size distribution, when applied as corrosion protection agents. These coatings were tested by using accelerated sulfuric acid spraying tests, both in dry and wet coating conditions. The coating adhesion ability and their microstructure were examined by the application of pull-off measurements and of SEM analysis, respectively and were found to present certain differences, regarding the adhesion ability and the surface morphologies. During the acid spraying procedure, the surface pH and the mass change of coated concrete specimens were recorded daily. The surface pH was reduced towards acidic values and the mass reduction approached almost  $-20\%$  in comparison with the initial coating mass for certain cases. Additionally, the hardness and roughness of concrete surface under the coating layer (i.e., the interface between the coating and the surface) after four days of acid spraying, exhibited much smaller changes (due to protection) in contrast to the uncoated concrete specimens (used as blank/comparison experiments), which were found to be highly affected/corroded. The formation of concrete corrosion and coating by-products, as noticed after the respective chemical reactions, was recorded by X-ray diffraction (XRD) measurements and the respective quantification of obtained results. In all the coated specimens only very small amounts of the major by-product (gypsum) was observed, indicating that the concrete surface was sufficiently protected from sulfuric acid attack.

**Keywords:** concrete corrosion and control; magnesium hydroxide coatings; sewerage pipe systems; acid spraying test



**Citation:** Merachtsaki, D.; Tsardaka, E.-C.; Anastasiou, E.K.; Yiannoulakis, H.; Zouboulis, A. Comparison of Different Magnesium Hydroxide Coatings Applied on Concrete Substrates (Sewer Pipes) for Protection against Bio-Corrosion. *Water* **2021**, *13*, 1227. <https://doi.org/10.3390/w13091227>

Academic Editor: Asbjorn Haaning Nielsen

Received: 29 March 2021

Accepted: 26 April 2021

Published: 28 April 2021

**Publisher's Note:** MDPI stays neutral with regard to jurisdictional claims in published maps and institutional affiliations.



**Copyright:** © 2021 by the authors. Licensee MDPI, Basel, Switzerland. This article is an open access article distributed under the terms and conditions of the Creative Commons Attribution (CC BY) license (<https://creativecommons.org/licenses/by/4.0/>).

## 1. Introduction

Several organic and inorganic coatings have been already widely used for the protection of concrete structures, aiming to prevent chemical agents (e.g., sulfuric acid, chlorides etc.), or even biological substances, from reaching and penetrating the concrete surface [1–3]. These substances can interact with the concrete surface, weaken the structural stability of concrete, and eventually, severely degrade it. The corrosion of concrete structures can occur under the influence of multiple factors, depending on the environmental etc. conditions prevailing around the structure [4]. The microbiologically induced corrosion (MIC) of

sewer pipes is considered a major problem for the urban sewerage systems, which has been studied since the mid-1940s and concerns the influence of specific microorganisms, which can develop on the inner surface of concrete pipes [5–7].

The wastewater that is discarded and transferred through the sewer pipes may carry several undesirable or even hazardous substances. The presence of sulfates in the wastewater stream can affect indirectly the progress of the MIC problem. Sulfates can be reduced into hydrogen sulfide, due to the chemical and biochemical processes and conditions that usually develop within the transferred wastewater. Then the hydrogen sulfide is emitted in the sewer pipe air phase, reaching the upper (usually empty) pipe area (also known as “crown”) and dissolves in the humidity film, existing onto the inner walls of pipes [8–10]. As a consequence, the acidity of dissolved hydrogen sulfide reduces the surface pH of concrete from the initial values 12–13 down to the value 9 [8]. By the time the pH value of the concrete surface falls below 9, the conditions become critical for the development of neutrophilic sulfur oxidizing bacteria (NSOB) [8,11]. These bacteria can subsequently oxidize the hydrogen sulfide on the concrete surface and produce the biogenic sulfuric acid, which lowers farther the surface pH of concrete. As a result, the colonization of surface by the acidophilic sulfur oxidizing bacteria (ASOB) may start, especially when the surface pH reaches acidic values close to 4 [8,12]. The so produced biogenic sulfuric acid attacks the alkaline components of the cement paste and forms gypsum ( $\text{CaSO}_4 \cdot \text{H}_2\text{O}$ ) and in some cases ettringite ( $3\text{CaO} \cdot \text{Al}_2\text{O}_3 \cdot 3\text{CaSO}_4 \cdot 32\text{H}_2\text{O}$ ) [10,12]. These by-products weaken and erode the concrete structure by consuming the cement paste and thus, reducing the thickness of concrete material [13,14].

Eventually, the MIC leads to the severe degradation of sewer concrete pipes and to the collapse of sewerage system, which in turn leads to costly pipe replacement [15,16], noting also that new/improved concrete materials have been developed, aiming to build a more durable sewerage network system, extending its operational life [17–19]. Nevertheless, the application of coatings can help the concrete pipes to preserve the main durability properties and mechanical strength, avoiding the need for frequent repairs and replacements. Several studies have been performed so far, regarding the use of protective coatings, applied on concrete surfaces, and in particular concerning the MIC protection, by using different types of material. The magnesium hydroxide-based coatings have already been examined as protective coatings, by using their ability to react with the biogenic-produced sulfuric acid, neutralizing its deterioration effect and avoiding the alternative reaction between the concrete surface and the acid [15,20]. However, the relevant research is rather limited, regarding the main anti-corrosive properties of these coatings [21], as well as their effect on the main parameters of protection processes (e.g., the properties of magnesium hydroxide powders, presenting different characteristics). Moreover, multiple methodologies, trying to simulate the MIC conditions, have been developed in order to evaluate the corrosion protection of coatings, or the corrosion of concrete surfaces [16,22,23].

The main objective of this paper is to evaluate the differences, if any, regarding the corrosion protection properties of five magnesium hydroxide coatings, presenting different physicochemical properties, aiming to improve their practicality aspects and elucidate better the respective protection mechanisms. A specifically designed and experimentally tested acid spraying procedure has been also developed to simulate the formation of sulfuric acid drops, which can be created onto the upper part (“crown”) of pipes, using a custom-made laboratory spraying chamber. Additionally, this study intended to evaluate the effect of dry and wet coating applications, on the anti-corrosive performance of coatings, by using the aforementioned accelerated sulfuric acid spraying test. The effect of different initial characteristics of powders, used for the composition of all five examined magnesium hydroxide coatings (i.e., the specific surface area and the pore size distribution), can influence the properties of the respective coatings’ formulations, regarding microstructure and adhesion ability. The anti-corrosive properties of these coatings were additionally evaluated by studying the formation of concrete corrosion by-products (e.g., gypsum etc.). The originality of this research is based mainly on the influence of dry and wet applications

of magnesium hydroxide coatings onto concrete specimens, as well as on the influence of specific surface area and pore size distribution of the initially used powders, regarding the main properties of prepared coatings, noting also that any relevant research has not been published so far.

## 2. Materials and Methods

### 2.1. Concrete Specimens

The preparation of concrete specimens is described in the Supplementary Material section (Text S1).

### 2.2. Surface Coatings

#### 2.2.1. Preparation of Magnesium Hydroxide Powders

Five different magnesium hydroxide (MH) powders were prepared in the laboratory by the controlled hydration of low and medium purity natural powder grades of microcrystalline caustic-calcined magnesia (CCM), provided by Grecian Magnesite S.A. (Gerakini, Greece). Table 1 summarizes the main properties of raw materials and the hydration conditions for the preparation of powders. The nominal MgO content of examined powders was determined by X-ray fluorescence elemental analysis, using a Spectro X-Lab 2000 instrument. The specific surface area (SSA) was determined by nitrogen adsorption, according to BET theory, using a Micromeritics Tristar Porosimeter. The powders were subsequently deagglomerated/milled using a centrifugal mill (Retsch ZM 100); the particle size of obtained powders was controlled using suitable mill screens.

**Table 1.** Raw materials (caustic-calcined magnesia, CCM) and the respective hydration conditions as applied for the preparations of magnesium hydroxide (MH) powders.

Powder	CCM			Hydration		
	Grade	MgO Content Nominal (%)	SSA (m <sup>2</sup> /g)	MgCl <sub>2</sub> (M)	MgAc (M)	Hours at 90 °C
C1	Low	82.34	17.7	0.015	0	3
C2	Low	82.34	17.7	0.015	0	3
C3	Medium, low reactivity	91.77	17.2	0.015	0	4
C4	Low	82.34	17.7	0	0.05	5
C5	Medium, high reactivity	90.30	46.8	0.015	0	3

The resulting magnesium hydroxide powders were characterized with the following parameters: particle size distribution (PSD), specific surface area and the major mineralogical phases. The particle size distribution measurements were performed by applying laser diffraction by wet dispersion, using a Helos/BR-Quixel Sympatec particle size analyzer. The mineralogical phases were determined by using an XRD Siemens Diffraktometer and the diffraction patterns were analyzed by the Rietveld methodology to obtain a semi-quantitative determination of the various mineralogical phases in the powders.

Table S1 (Supplementary Material) summarizes the main mineralogical phases of prepared magnesium hydroxide powders, according to the results of the quantification of XRD diffraction patterns. The composition of each magnesium hydroxide powder, determined by XRF elemental analysis, is presented in Table 2. The specific surface area, the particle size distribution and the total alkalinity of all magnesium hydroxide powders are presented in Table 3.

**Table 2.** Composition of five magnesium hydroxide powders (%).

Material	MgO	SiO <sub>2</sub>	CaO	Fe <sub>2</sub> O <sub>3</sub>	Al <sub>2</sub> O <sub>3</sub>	SO <sub>3</sub>	LOI
C1	63.49	8.77	2.30	0.15	0.15	0.11	25.03
C2	63.15	8.73	2.29	0.15	0.15	0.11	25.42
C3	66.54	3.05	1.48	0.07	0.07	0.09	28.70
C4	61.91	8.80	2.31	0.15	0.15	0.11	26.57
C5	65.00	3.32	1.52	0.08	0.05	0.14	29.90

**Table 3.** The main physicochemical characterization parameters (i.e., total alkalinity, specific surface area (SSA) and particle size distribution (PSD)) of examined magnesium hydroxide powders.

Material	Total Alkalinity (%)	SSA (m <sup>2</sup> /g)	PSD (μm)	
			d <sub>50</sub>	d <sub>90</sub>
C1	58.2	13.1	17.80	69.1
C2	59.0	18.7	8.40	29.5
C3	63.5	11.2	10.54	39.9
C4	59.8	13.2	9.54	40.8
C5	62.6	32.3	9.90	38.1

The different MH powders vary in their composition, concerning the mineralogical phases, as well as the magnesium content (expressed as oxide %), the total alkalinity, the specific surface area and the particle size. The total alkalinity is an important indicator of each powder's active content towards the neutralization reaction with acid (e.g., sulfuric) and can be estimated roughly as the sum of MgO equivalent content for all the present reactive phases, according to the following empirical equation; noting also that the periclase corresponds to the non-hydrated caustic calcined magnesia:

$$\text{Total Alkalinity (\%)} \approx \text{Brucite} \times (40.3/58.3) + \text{Periclase} + \text{CaO} \times (40.3/56) \quad (1)$$

In order to confirm the respective alkalinity results, the neutralization reaction of all magnesium hydroxide powders was also performed, by using a sulfuric acid solution (0.4 M). The titration results (see Figure S1, Supplementary Material) are in good agreement with the calculated total alkalinity data (Table 3).

As can be noticed from the characterization of prepared powders, C1 and C2 samples are essentially the same (i.e., using the same raw material and same procedure as can be seen from Table 1), differing only in the particle size, with the C2 considered as the finer equivalent of C1, due to the application of stricter de-agglomeration/milling. This fact also affects the specific surface area, which was observed to be increased in the C2 sample. On the other hand, the C4 sample, due to the application of longer hydration time and to the use of different and higher concentration of hydration agent (i.e., magnesium acetate), leading to higher conversion, presents higher brucite (magnesium hydroxide content) and lower periclase (MgO) content, than the C1 and C2 samples; noting however, that all these powders exhibit similar total alkalinity.

The C3 sample was produced from a higher purity raw material; hence, it presents higher magnesium hydroxide content and alkalinity, despite the similarity of applied conditions with the C1 and C2 samples.

The C5 sample was also produced from a higher purity and higher SSA raw material (Table 1), leading to a powder with significantly higher magnesium hydroxide content and higher surface area (32.3 m<sup>2</sup>/g) with respect to the similar C3 sample (11.2 m<sup>2</sup>/g).

### 2.2.2. Preparation of Coatings

The resulting slurries/coatings were named after the respective powders. Methylcellulose was added in the mixtures as an adhesion promoter agent, because the magnesium hydroxide slurries present low to zero adhesion on concrete. According to a previous

relevant study [21] the addition of 0.4% wt. content of methyl-cellulose can offer sufficient adhesion ability to the magnesium hydroxide coatings; therefore, this amount of cellulose was also selected for this study. Deionized water was added for the preparation of all coatings, resulting in slurries with 57.5% wt. content of solids. In order to maintain reduced viscosity of the slurries and to improve the workability of pastes, as well as to enhance their stability, a common dispersant polymer for mineral slurries (Acumer 9300) was also added at 1.5% wt. of solids.

For the preparation of slurries, deionized water was heated at 90 °C. Then, the methyl-cellulose and the dispersant polymer were added, under stirring. When the solutions cooled at room temperature, the respective MH powders were added and mixed under mechanical stirring for at least 1 h, until the slurries become homogenous. After that the coatings were applied onto the concrete specimens, as described in the respective procedures.

The thickness of applied coatings was selected, according to the relevant literature and to preliminary testing, ranging between 1.0–1.5 mm [3,21,24]. In order to achieve uniformity between the coatings, the thickness was expressed according to the specific amount of applied coating, i.e., 0.0018–0.0020 g/mm<sup>2</sup>. The coatings were then dried for 3 days under normal laboratory conditions (i.e., 21 ± 2 °C and relative humidity 60 ± 10%) before testing, except for the case of wet coating application, where the coated specimens were tested immediately (i.e., without the previous drying step).

The proper application of a coating onto a surface depends mainly upon its sufficient adhesion with the substrate. In that way, the respective coatings were evaluated for their adhesion ability onto the concrete surface, with the application of pull-off bond testing method, according to the standards EN 1542:1999 [25] and EN 13578:2003 [26]. Concrete specimens with dimensions 200 mm × 200 mm × 20 mm were used as substrate for the application of coatings and for performing the respective measurements. Two concrete specimens, with the aforementioned dimensions, were tested for each magnesium hydroxide coating, with four testing areas on each specimen (i.e., totally eight testing areas for each coating) (see Figure S2, Supplementary Material). The pull-off equipment (digital pull-off strength tester, Matest) was used in order to proceed with the recording of failure load, as well as with the type of failure.

### 2.3. Scanning Electron Microscopy (SEM) Analysis

Scanning electron microscopy (SEM) analysis was used to provide a closer examination of the concrete-coating interfaces and the different microstructure of examined coatings. Moreover, specific information, regarding the magnesium content in the concrete structure, can be obtained by using energy-dispersive X-ray spectroscopy (EDS) microanalysis. The coated specimens were cut perpendicular to the coatings' surface, so that the concrete-coating interface could be observed. After that the profile surfaces were polished, resulting to clear observation of the achieved flat surfaces for further study. All surfaces were coated with carbon, using a Jeol JEE-4X carbon vacuum evaporator. A scanning electron microscope JEOL JSM-6390LV (JEOL, Tokyo, Japan) was used for the micrographs, with an accelerating voltage 20 kV and beam current 45 nA. Also, the EDS analysis was performed by using an INCA Energy X-ray microanalysis system.

### 2.4. Sulfuric Acid Spraying Tests

The magnesium hydroxide coatings can offer protection to the concrete surfaces against bio-corrosion by employing two major mechanisms. The first is by preserving the stability of alkaline pH surface values at the surface and by blocking the development of sulfur oxidizing bacteria, while the second mechanism is by reaction with the biogenic sulfuric acid, leading to its neutralization, in case the microorganisms can eventually develop on the concrete's surface and create biogenic sulfuric acid.

Two different accelerated sulfuric acid spraying tests were applied, in order to study the anti-corrosion properties of MH coatings in relatively short time period. In particular, the first accelerated acid spraying test was performed by using a hand-held spraying device

(i.e., manually), while the second acid spraying test was performed by a custom-made spraying laboratory chamber (i.e., automatically). In the latter test, two methods for the application of coatings were examined, i.e., a dry and a wet one. In the first case (dry method), the coatings were applied and left to dry for 3 days under normal laboratory conditions before the sulfuric acid spraying applications, while in the second case (wet method) the coated concrete specimens were subjected immediately to acid spraying tests, i.e., without any preliminary drying step. These two practices were performed, aiming to determine whether the preliminary drying of coatings may influence their protective role against the concrete corrosion. Four concrete specimens were examined for each coating case daily, in order to perform these tests. The concrete specimens with dimensions of 50 mm × 50 mm × 20 mm were used for the acid spraying tests, but only one side of each specimen was coated (i.e., the larger, 50 mm × 50 mm).

Sulfuric acid solutions with different concentrations were used in each acid spraying test. However, in both tests the same principles were used for the calculation of the corresponding necessary sulfuric acid amount to be sprayed; the stoichiometry calculations were performed according to [21]. Additional information regarding the stoichiometry calculations is given in Supplementary Material (Text S2). The number of spraying days was selected to be four in both accelerated tests, in order to be able to perform rapid testing procedures and to examine multiple magnesium hydroxide coatings. Therefore, the respective stoichiometry (i.e., the moles of sulfuric acid) was divided by the number of spraying days and the daily spraying application stoichiometry corresponded to 25% of the overall stoichiometry of the respective neutralization reaction between the coatings and the sulfuric acid. The difference between the two accelerated spraying tests was the number of daily spraying applications, due to the different initial acid solutions concentrations used for each case.

A flat surface pH electrode (Extech PH100: Waterproof ExStik pH meter, Extech Instruments) (Extech Instruments, Nashua, NH, USA) was used to record the surface pH values of specimens. The starting values of surface pH were recorded for each specimen before the beginning of acid spraying. The surfaces to be measured were wetted with 1 mL of deionized water prior to the measurement.

#### 2.4.1. First Acid Spraying Test

The first sulfuric acid spraying test was performed by using a hand-held device and spraying a sulfuric acid working solution (4 M). Each day, the specimens were removed from the acid spraying procedure and examined, in order to record the pH, the thickness, the mass change and the major mineralogical changes/phases (see Section 2.5). A climatic test chamber was used for the storage of the samples, between the spraying applications, simulating common sewer pipe conditions (i.e.,  $20 \pm 2$  °C and 99% relative humidity).

The mass changes of concrete specimens were recorded daily by using an electronic balance Kern PCB 4000-2 ( $4.000 \pm 0.001$  g). The daily mass measurements were conducted to evaluate the mass changes, which correspond mainly to the consumption of coatings, due to the neutralization reactions with sulfuric acid.

The thickness of coatings was measured by using a destructive technique in this preliminary acid spraying test. A Dino Lite Digital Microscope was used to photograph the cross-section of the coated concrete specimens. The microscope's software can calculate the thickness, according to the magnification used in each picture. The thickness was measured on the coated concrete specimens before and after the application of acid spraying in order to examine the consumption of coating.

#### 2.4.2. Second Acid Spraying Test

The concentration of sulfuric acid solution in the previous (accelerated) sulfuric acid first spraying test was quite high (4 M), in order to magnify the effect of acid on the coating properties and consumption. However, the common conditions, regarding sulfate concentration, existing in a sewer pipe, are rather milder. Therefore, after the quite extreme

acidic conditions applied during the first accelerated spraying test, another acid spraying test, using much lower concentration of sulfuric acid solution, was performed. In the second acid spraying test a 0.2 M sulfuric acid solution was used and sprayed onto the coated concrete specimens. A custom-made poly(methyl methacrylate) chamber (Figure 1) was used for this test, equipped with nebulizers, which could properly spray sulfuric acid on the surface of coated concrete specimens. The conditions in the chamber were also closer to simulate the usual sewer pipe conditions, i.e., maintaining the temperature at  $20 \pm 2$  °C and 99% relative humidity.



**Figure 1.** Custom-made acid spraying chamber equipped with nebulizers, spraying the surface of coated concrete specimens with the sulfuric acid solution (0.2 M).

The results of surface pH values, regarding the coated concrete specimens, as well as of the mineralogical analysis of the main crystalline phases, existing on the specimens' surface, were compared with the respective results of the first acid spraying test. As mentioned in Section 2.4, the application of coatings in this chamber test was examined in two ways, i.e., dry and wet coating applications.

The corrosion of concrete surface may lead to changes of the surface hardness and roughness. In order to record these properties, the specimens were examined before and after acid spraying. Additionally, the same properties of uncoated concrete specimens were also measured for reasons of comparison, i.e., before and after acid spraying. The measurements of coated samples were conducted after the coating was removed from the concrete surface. The hardness measurements were performed with a Shore A, hardness tester (Sauter), which was adapted on a test stand with glass base plate, in order to conduct the measurement. An electronic portable roughness gauge, Rugosurf 20 (Tesa), was used for the roughness measurements, and the corresponding results were recorded in Ra ( $\mu\text{m}$ ), being the arithmetic average height from the average (mean) line. Both parameters are presented in relative values and in respect to the initial values of concrete specimens (i.e., before the acid spraying).

### 2.5. X-ray Diffraction (XRD) Analysis

The coated concrete specimens, sprayed according to the previous procedures (Sections 2.4.1 and 2.4.2), were used for the determination of major mineralogical phases. After finishing the acid spraying tests, the specimens were dried at 40 °C for 24 h and

then, superficial samples scratched from the top of specimens, ground and measured. The structural phases (mineralogical composition) of the so obtained samples were analyzed by XRD measurements, using a PW 1840 Phillips diffractometer with CuK $\alpha$  radiation, step size of 0.02° and step time of 0.4 s, operating at 30 kV and 10 mA. The diffractograms obtained were quantified by following the Rietveld methodology, using the FullProf Suite Software.

### 3. Results

#### 3.1. Adhesion Measurements

The efficient adhesion of coatings onto the concrete substrate evaluated for all examined coatings by using the pull-off measurements. In order to calculate the tensile bond strength, the values of failure load, resulting from the pull-off measurements, were used, according to the aforementioned standards [25,26] and to the following equation:

$$f_h = 4F_h / \pi D^2 \quad (2)$$

where  $f_h$  is the tensile bond strength of the specimens (MPa),  $F_h$  is the failure load (N),  $D$  is the mean diameter of test specimen (mm) [25].

The tensile bond strength between the applied coatings and the concrete substrate, as well as the type of failure is presented in Table 4. Two concrete specimens, with four testing areas in each one, were used for the evaluation of each sample coating. There are two types of coating failure that can be optically observed and defined; the first type of failure is the adhesion failure between the concrete and the coating, type A/B (%) (see Figure S3a, Supplementary Material), and the second type is the cohesion failure within the layer of coating itself, type B (%) (see Figure S3b, Supplementary Material). Additionally, the combination of these two types can be also observed. The results are usually expressed as a percentage, based on the surface area. The indicated values of A/B (%) and B (%) type of failures are the average of eight testing areas, noting that large dispersion of obtained results was not observed, as rather similar values were recorded for each coating sample.

**Table 4.** Tensile bond strength ( $f_h$ ) values, the respective standard deviation (SD) and the type of failure of coatings.

Coating	$f_h$ (MPa)	SD (MPa)	Type of Failure	
			A/B (%) <sup>1</sup>	B (%) <sup>2</sup>
C1	0.36	0.054	27.5	72.5
C2	0.31	0.052	32.5	67.5
C3	0.42	0.055	96	4
C4	0.24	0.031	0	100
C5	0.13	0.029	4	96

<sup>1</sup> Adhesion failure between the substrate and the coating layer. <sup>2</sup> Cohesion failure within the layer of coating.

The results showed that even though the same amount of methylcellulose was added in every magnesium hydroxide composition, the adhesion ability of the respective coatings was different. The coating C3 presented the highest tensile bond value (0.42 MPa), while the C5 coating presented the smallest value between all coatings (0.13 MPa). Additionally, the coatings C1, C2 and C4 exhibited intermediate tensile bond values, i.e., 0.36, 0.31 and 0.24 MPa, respectively. However, the tensile bond strength should be combined with the specific type of failure in order to understand better the adhesion ability of each coating.

In the case of intended application, the lowest values of A/B (%) are more important for the attachment ability of coatings onto the concrete surface, than the B (%) values. In that way, the adhesion of coatings onto the concrete substrate is larger than the cohesion failure within the coating layer. It is obvious from the results of failure type in Table 4, that the coating C3 exhibited the largest adhesion failure between all coatings (96% A/B). As far as the coatings with the minimum A/B (%) values are concerned, the coating C4 presented zero adhesion failure and the C5 coating follows with only 4% adhesion failure, showing

the high ability of these coatings to adhere efficiently onto the concrete surface and thus, their greater stability. Additionally, the coatings C1 and C2 exhibited satisfactory adhesion with the concrete substrate because they presented relatively high B type of failure (72.5% and 67.5%, respectively).

To sum up, the high tensile bond of coating C3 is not enough to conclude that this coating had the best adhesion ability between the examined coatings. It can be assumed that the coatings C1 and C2 presented satisfactory adhesion (tensile bond strength), in combination with the desirable type of failure. The higher tensile bond strength of the C3 coating is relevant probably with its improved microstructure.

### 3.2. SEM Analysis

SEM was used for the further/closer examination of coatings-concrete interface, as well as for the coatings' microstructure. Moreover, the penetration of coatings into the concrete substrate/structure was verified by using the EDS supplementary analysis. All coatings remained well attached onto the concrete substrate during the preparation process (i.e., during the cutting and polishing procedures), whereas the microstructure of interfaces was also studied before the application of spraying tests.

In Figure 2 the SEM micrographs of two (selected) magnesium hydroxide coatings onto the concrete surfaces can verify their adhesion ability. The respective micrographs of the coatings C1, C3 and C5 are presented in Supplementary Material (see Figure S4). The structures of the coatings and of the concrete surface, present different roughness and porosity and thus, they are distinct. The concrete surface is compact and its structure is dense, with some large open pores as showed in Figure 3, while the scratch polishing lines can be noticed on every examined concrete surface. It must be noted that the used concrete MC (0.45) is considered as a good quality concrete of relatively low porosity. The coating-concrete interfaces are presented to be really firm, without any voids or cracks, indicating the absence of regional adhesion problems. The coating thickness ranged between 0.8–1.5 mm, according to these observations. The coating structure seems to be porous and loose, in contrast to the structure of concrete.

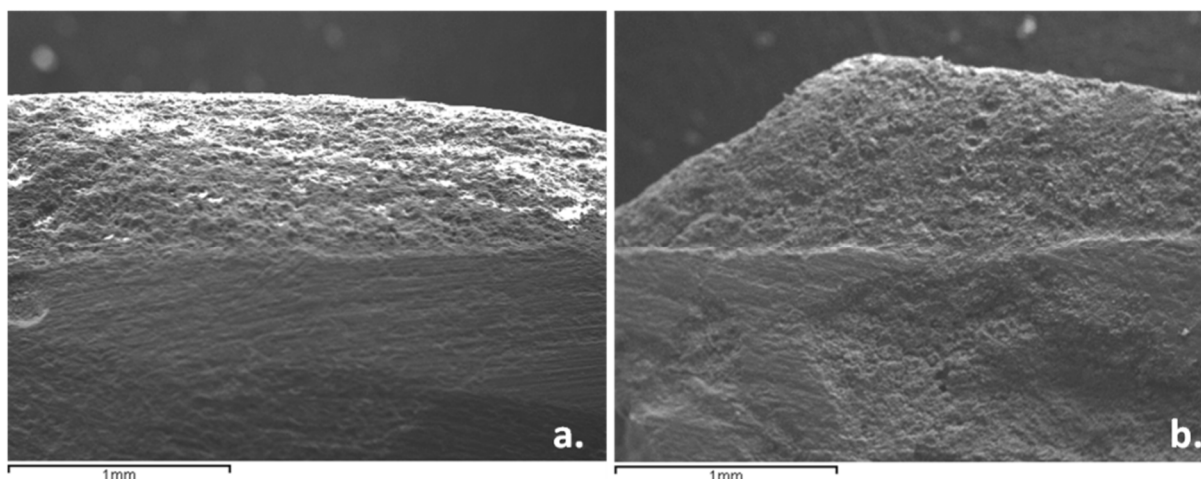


**Figure 2.** Scanning electron microscopy (SEM) micrographs of coated concrete specimens with the coatings; (a) C2 and (b) C4. The coatings are presented in the upper side, whereas the concrete is presented in the lower side of each image.

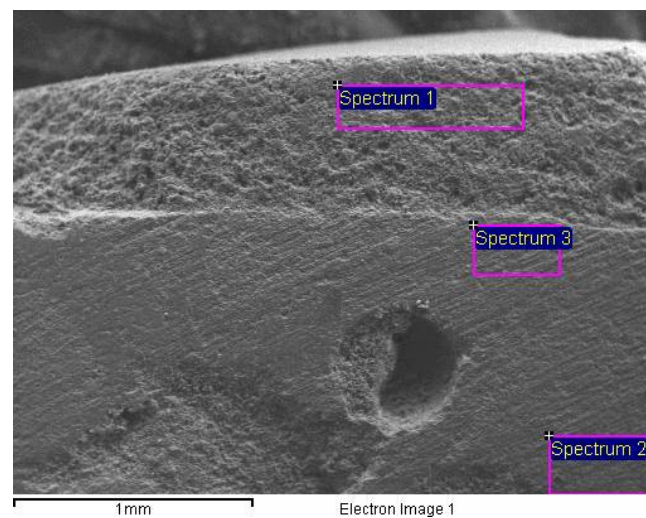


**Figure 3.** SEM-micrographs of the concrete specimen coated with the coating C3, also showing the respective energy-dispersive X-ray spectroscopy (EDS) spectra.

Even though the coatings adhered firmly onto the concrete surface and a rather uniform interface was created, the texture of the interface in sample C3 was found to be different and weaker (Figure 4). The respective micrographs of the coatings C1, C4 and C5 are presented in the supplementary material (see Figure S5). Figure 4a depicts the interface between the coating C2 and the concrete surface. In this case, the coating presents a homogenous distribution of pores and there is absence of defaults close to the interface. Figure 4b depicts the interface between the coating C3 and the concrete surface, showing a more compact coating, than in the case of C2. Nevertheless, the micro-pores are not well distributed, as they are observed close to the interface in greater proportion, than in the upper structure. As a result, the increased micro-porosity of interface in this case may create a regional weaker zone for the coating C3.

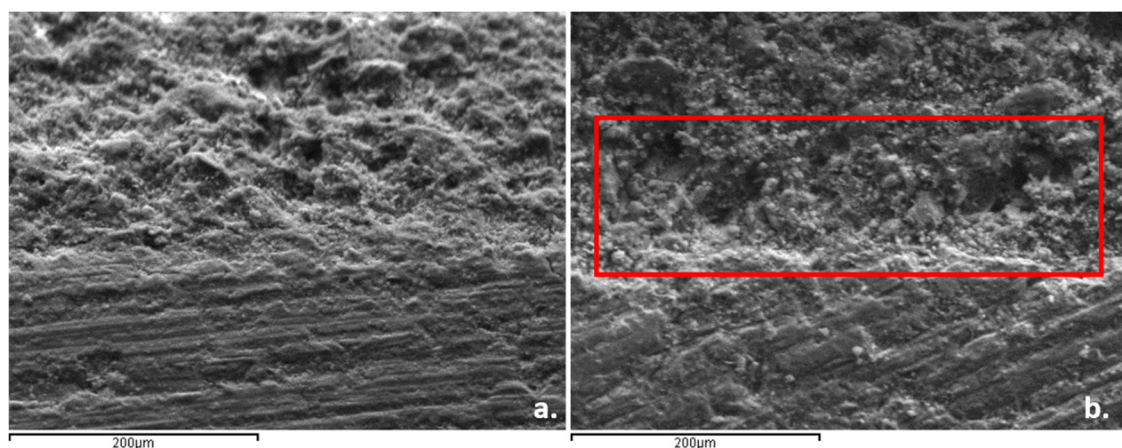


**Figure 4.** SEM micrographs of the coating-concrete interfaces for the concrete specimens coated with the coatings; (a) C2, and (b) C3.

Additionally, the designated spectrum areas of EDS microanalysis (Figure 3), as presented in Table 5, show the penetration of magnesium into the structure of concrete. Three spectrum areas were analyzed: (a) Spectrum 1, representing the coating surface, (b) Spectrum 2, representing the concrete surface, but far from the interface, and (c) Spectrum 3, representing the concrete surface, but closer to the interface, aiming to evaluate the penetration of magnesium into the concrete structure. The EDS analysis showed that the Mg content was 89.92% wt. for the case of coating, 1.56% wt. for the concrete substrate and

3.37% wt. for the concrete near the interface with coating (in the depth of 200  $\mu\text{m}$ ). These results indicate that a small amount of magnesium coating can penetrate into the concrete at the depth of several  $\mu\text{m}$ .

**Table 5.** EDS spectra of coating C3 and of concrete substrate, closer to the interface, as well as far from the interface, presented in Figure 3.

Elements	Weight %		
	Spectrum 1	Spectrum 2	Spectrum 3
Mg	89.92	1.56	3.37
Si	5.93	1.36	16.00
Ca	4.14	97.09	80.63

As far as the roughness of microstructure for the examined coatings is concerned, in Figure 5 a high magnification of all five coatings is presented. The coatings C1, C3, C4 and C5 seem to form many smaller particles on their surface, creating a much rougher surface, than the coating C2, which seems to be composed from larger size particles. The C2 coating sample presents a denser morphology and a smaller micro-porosity. When compared to the C1 sample (noting that they differ only in particle size) it can be concluded that the particle size of used powders can significantly affect the morphology of each coating. Additionally, the structure of coatings C1, C3, C4 and C5 is loose and porous, with the formed micro-pores quite homogeneously distributed. This fact may also affect the diffusion of sulfuric acid, during the subsequent acid spraying tests.

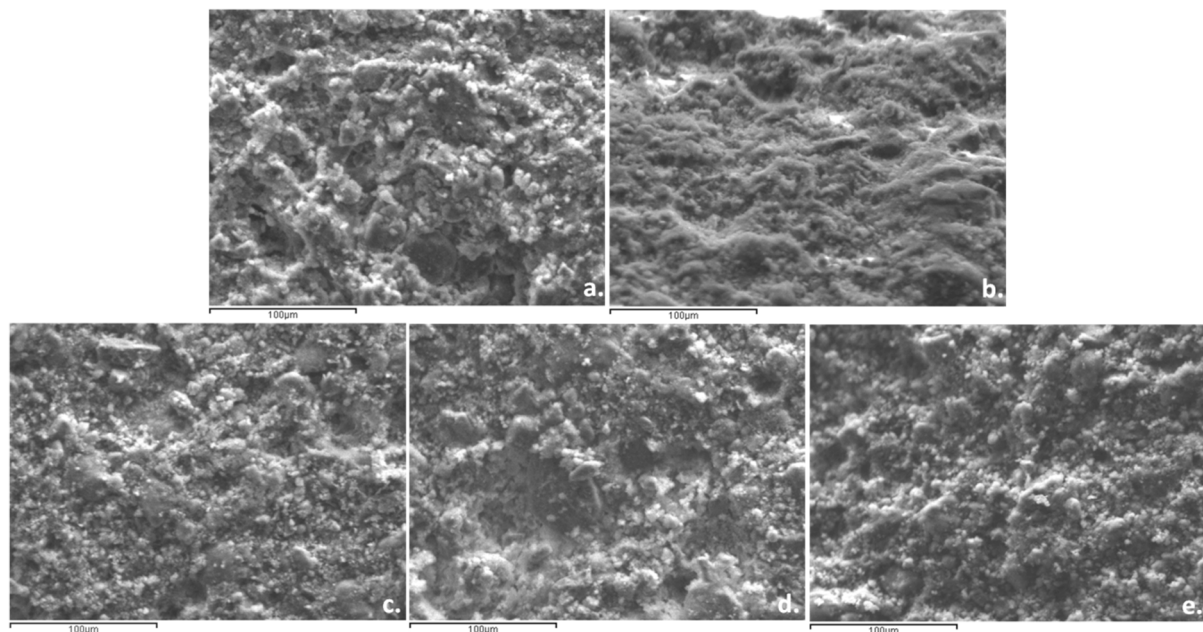


**Figure 5.** SEM-micrographs of coatings microstructure by using high magnification for the examined coatings; (a) C1, (b) C2, (c) C3, (d) C4, and (e) C5.

### 3.3. Accelerated Acid Spraying Tests

#### 3.3.1. First Acid Spraying Test

As mentioned in Section 2.4, the capacity to maintain sufficiently alkaline pH values in the internal surface of concrete pipes is very important, regarding the efficient application of coatings in the sewerage network. In this way, the coatings can block the growth of neutrophilic and (later) of acidophilic sulfur oxidizing bacteria, hence blocking the production of biogenic sulfuric acid. In particular, the coatings can maintain the alkaline pH values of the concrete surface by reacting with the (biogenic) sulfuric acid and eventually would be

consumed, due to the respective neutralization reactions. In contrast, the uncoated concrete specimens present a much higher reduction of surface pH values towards neutral or acidic pH values, due to the formation of corrosion by-products (mainly gypsum).

The results of surface pH values (daily recordings) are presented in Figure 6. The initial pH values of coated and uncoated concrete specimens were found to be between values 9 and 10. These decreased pH values of uncoated specimens, in comparison to the usual pH values of concrete surface, being between 12 and 13, indicate that surface carbonation took place [13]. After the initiation of the acid spraying process, the pH values of coated specimens were slightly decreased, although they still preserved their initial alkaline pH values, throughout the spraying process, as they ranged between 8 and 10 for all cases, whereas the uncoated concrete specimens' surface pH reached the value 5. According to these results, the coating C4 presented a slightly higher pH decrease, in comparison to the other coatings, but all coatings performed in quite a similar manner.

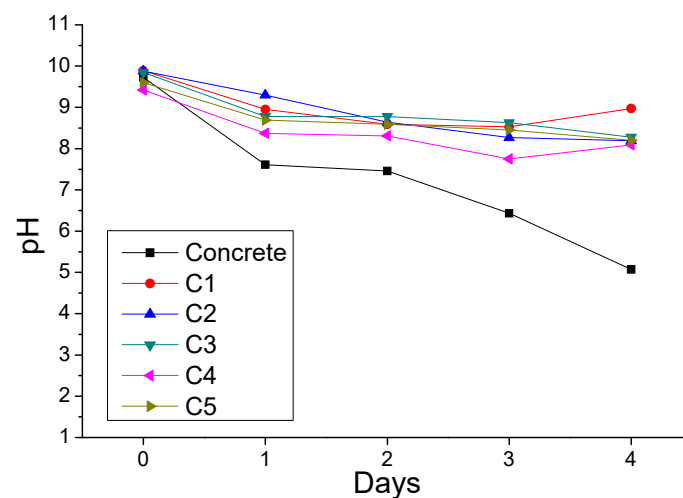


**Figure 6.** Surface pH values of coated and uncoated concrete specimens, during the application of the first acid spraying test.

All specimens were sprayed daily with 25% of the respective reaction's stoichiometry, using a concentrated sulfuric acid solution (4 M) for 4 days. Each day, four specimens of each coating sample were removed from the spraying process and were examined, regarding mass and thickness changes, as well as regarding the main crystalline phases (by XRD). Day 0, as indicated in the figures, corresponds to the initial surface pH values of the coated and uncoated concrete surface.

The coatings were expected to be fully consumed after the 4th spraying day, according to the respective stoichiometry calculations. However, part of the applied coatings continued to remain onto the concrete surface, even after the four days of acid spraying. A possible explanation may be that the sprayed amount of sulfuric acid, corresponding to the total coating amount, could reach (and react) only with the exposed coating surface, instead of the whole quantity of the coating mass. Figure S6 depicts the concrete specimens coated with different coatings, after four days of acid spraying.

To monitor better the consumption of coatings, the mass changes of coated specimens after each day of acid spraying test (totally four), were measured against their initial mass (Figure 7). Note, however, that two opposite processes can affect the mass change of specimens, i.e., the consumption of coating, due to the neutralization reaction with acid, leading to mass decrease, and the formation of corrosion by-products, e.g., gypsum, leading to mass increase. Even though some coated specimens (coated with the C2, C4, and C5 samples) gained weight at the beginning of acid spraying, due to the possible formation of by-products, the mass of specimens was finally decreased, due to the eventual consumption of the coating. The coatings C1 and C3 started losing weight immediately

after the first day of acid spraying, which is preferable, than the formation of by-products, formed in the case of other coatings. Finally, the largest coating consumption was observed for the coatings C3 and C4.

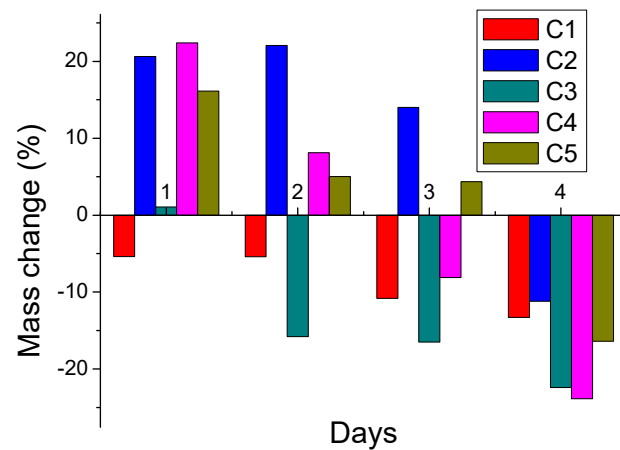


**Figure 7.** Mass changes of examined coatings, during the application of the first acid spraying test.

The consumption of coatings can be monitored also by using the change of coatings' thickness after four days of acid spraying test. Figure 8 presents the evolution of coatings' thickness during the acid spraying process. The decrease of thickness indicates the consumption of coatings, due to the neutralization reaction with sulfuric acid, and can also verify the protection mechanism, by inhibiting the reaction between the concrete and the sulfuric acid. The coating C3 presented the greatest reduction of thickness, whereas the other coatings presented rather similar reduction behavior.

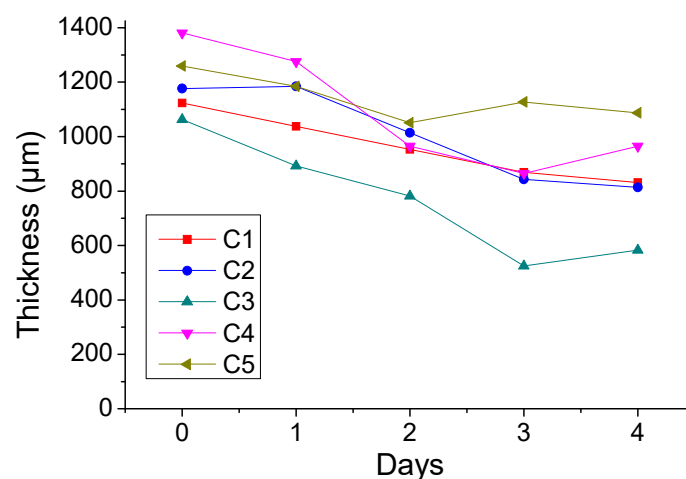


**Figure 8.** The evolution of coatings' thickness during the application of the first acid spraying test.

### 3.3.2. Second Acid Spraying Test

As described in Section 2.4, apart from the acid spraying test using the hand-held device, another test was performed, using a custom made acid spraying laboratory chamber, denoted as the second acid spraying test. Additionally, the coated specimens were tested both in dry and wet conditions. In that way, the results are presented separately for the two different conditions. In the second acid spraying test, a 0.2 M sulfuric acid solution was sprayed onto the coated and the uncoated surface of concrete specimens. The surface pH values of dry and wet samples are shown in Figure 9. Uncoated concrete specimens were the same for either dry or wet coating applications. Day 0 corresponds to the initial surface pH values of the coated and of the concrete (uncoated) surfaces.

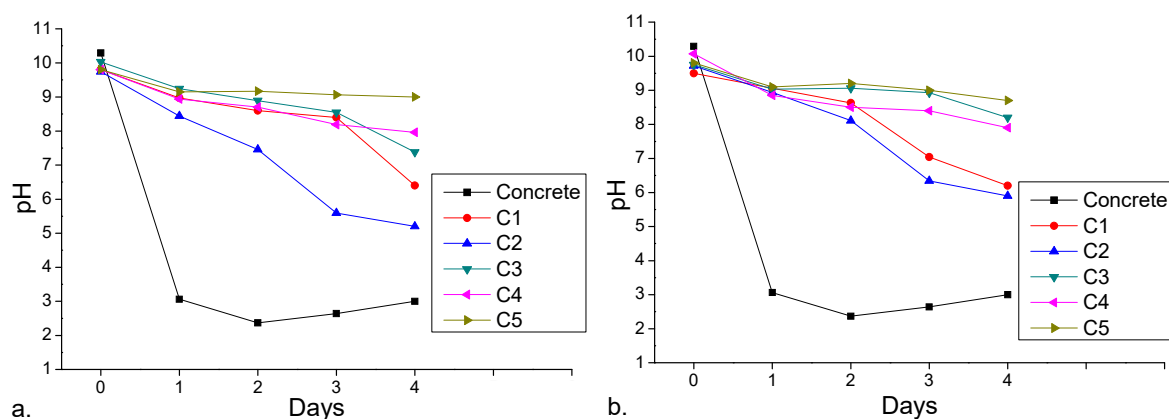


**Figure 9.** Surface pH values of coated and uncoated concrete specimens; (a) dry and (b) wet coating applications, during the application of the second acid spraying test.

Despite the fact that the applied concentration of sulfuric acid is substantially lower in the second spraying test, than in the first one, the surface pH of coatings reached lower (i.e., circa neutral) values, as compared with the results obtained from the first test (see Figure 6). This observation can be dedicated to the fact that the number of daily spraying applications during the second spraying test was much higher, than in the first one, in order to achieve the selected daily stoichiometry of neutralization (i.e., 25% of the respective reaction). Consequently, the frequency of spraying applications in this case was considerably higher and the overall conditions of acid attack were more intensive, as compared to the first test. However, some of the coatings were still capable to maintain sufficient alkaline pH values even under these experimental conditions (i.e., the samples C3, C4 and C5), with the exceptions of coatings C1 and C2, in both dry and wet coating conditions. In contrast, the uncoated concrete specimens presented very low (acidic) surface pH values, because the sulfuric acid was sprayed onto the unprotected concrete surface in higher frequency, than in the first acid spraying test. In that way, the sprayed sulfuric acid was in excess on the specimen surface, hence resulting to the further decrease of surface pH values in comparison with the first test.

The surface hardness and roughness measurements on both dry- and wet-coated concrete specimens were conducted after the second acid spraying test and after the coatings were appropriately removed from the specimens' surfaces. For the uncoated specimens the same properties were also measured. These results are shown in Figures 10 and 11, regarding the hardness and roughness changes, respectively.

It is obvious from the results shown in Figure 10 that the uncoated concrete specimens presented a gradual reduction of surface hardness during the spraying procedure. The reaction between the concrete (i.e., the hardened cement paste of concrete) and the sulfuric acid can lead to the formation of gypsum and affect significantly the surface properties. Furthermore, the results concerning the coated specimens were different for each coating case. The relatively higher change of surface hardness in the specimens coated with the C2 coating (for dry:  $-13.75\%$ , for wet:  $-14.6\%$ ) after four days of spraying indicates the possible diffusion of sulfuric acid through the coating. In this way, the sulfuric acid can reach the concrete surface despite the coating's presence and subsequently, can affect the surface characteristics of concrete. The rest coated specimens (i.e., samples C1, C3, C4 and C5) exhibited smaller hardness reduction, both in dry and wet conditions, than the samples coated with the C2 coating and the uncoated concrete sample after 4 days of spraying, indicating their ability to offer sufficient protection of the concrete substrate. Among them, coating C4 presented smaller deviations.

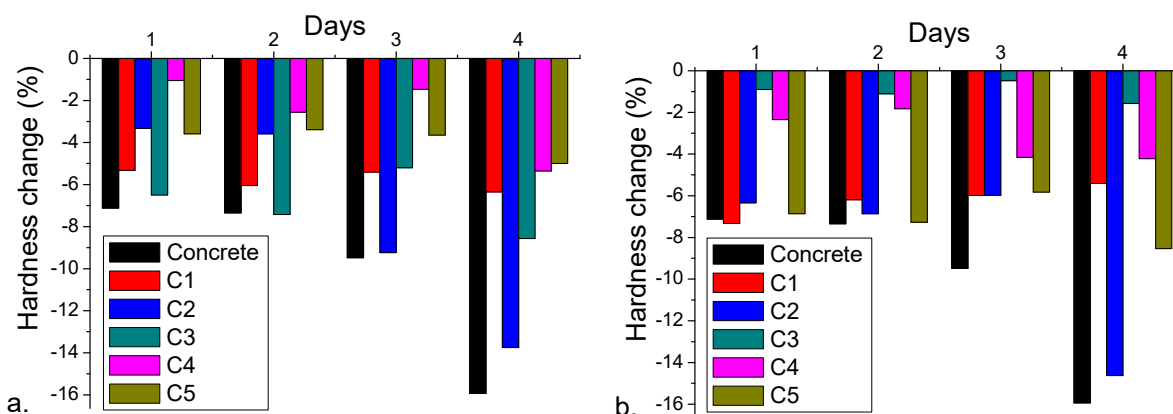


**Figure 10.** The change of hardness for coated and uncoated concrete specimens, during the application of the second acid spraying test; (a) dry and (b) wet coating applications.

Comparing the behavior of C3 coating between dry and wet coating applications, the results are different, because during the dry conditions the hardness of samples seemed to be affected, while during the wet conditions the change of hardness was found to be substantially smaller. This shows that the sulfuric acid can penetrate through the dry C3 coating (possibly through voids and capillaries), but this procedure is blocked/hindered during the application of wet conditions. To sum up, the magnesium hydroxide coatings, apart from the coating C2, can protect sufficiently the concrete surface from degradation (due to corrosion) and the specific conditions of coating application (i.e., dry or wet) may significantly affect the coating performance, depending also on the specific environmental conditions.

As depicted in Figure 11, the roughness of uncoated concrete specimens was rapidly increased after the first day of spraying process and continued to increase throughout the test. As mentioned before, the reaction of cement paste with the sulfuric acid, leads to the formation of gypsum. Gypsum is a pastry white mass that can be easily washed off, resulting in the exposure of concrete aggregates, hence increasing the surface roughness of these specimens.

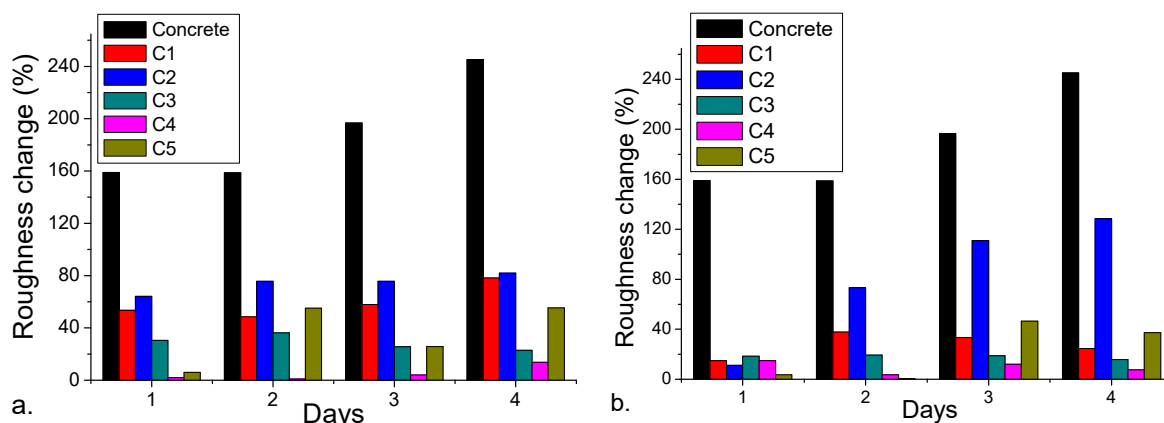


**Figure 11.** The change of roughness for coated and uncoated concrete specimens during the application of the second acid spraying test; (a) dry and (b) wet coating applications.

Even though the roughness of coated concrete specimens was also increased, however the respective values for all cases were found to be smaller, than the half of relevant change for the uncoated specimens' roughness. In particular, the coated specimens with the C3 and C4 samples presented small and rather stable surface roughness, suggesting that they can offer sufficient corrosion protection to concrete substrate. These results are also in good agreement with the respective hardness results. The coatings C1 and C5 also seemed to protect substantially the concrete specimens, because they exhibited also smaller roughness

changes during the second acid spraying procedure. The specimens coated with the coating C2 exhibited the largest roughness change, of all the examined coated specimens, mainly in the case of wet conditions (Figure 11b). To sum up, the examined magnesium hydroxide coatings seemed to generally prevent the degradation of concrete, in terms of roughness change, although to a different degree.

### 3.4. XRD Analysis

#### 3.4.1. First Acid Spraying Test

An overlay of the XRD diffractograms, regarding the examined coatings (C1–C5), as well as of the uncoated concrete specimens, is presented in Figure 12. In particular, these diffractograms represent the respective samples before (Figure 12a) and after 4 days (Figure 12b) of sulfuric acid spraying with a 4 M sulfuric acid solution (i.e., when applying the first acid spraying test).

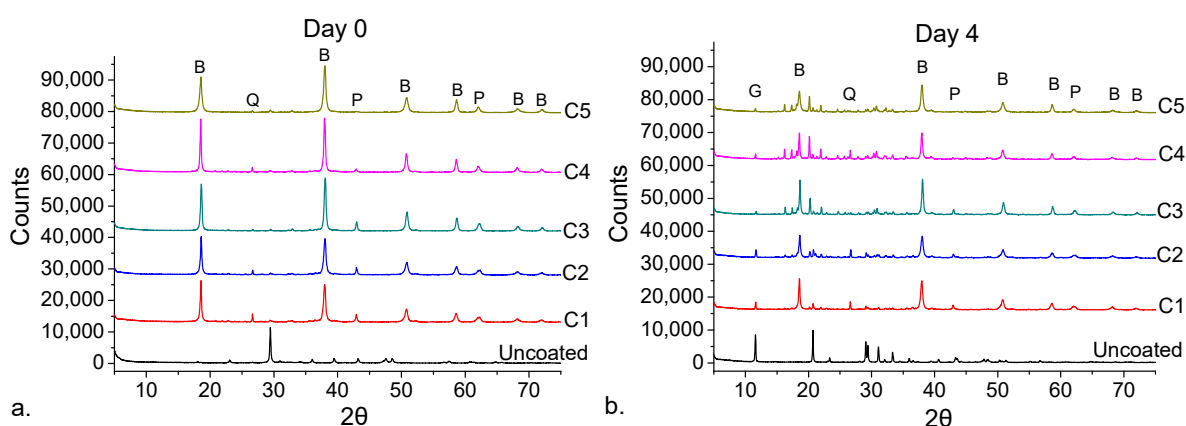


**Figure 12.** X-ray diffraction (XRD) overlay diffractograms of coated and uncoated concrete specimens; (a) before (day 0) and (b) after 4 days of the application of the first acid spraying test; G: Gypsum, P: periclase, B: brucite, Q: quartz.

The main peaks of periclase ( $\text{MgO}$ ), brucite ( $\text{Mg}(\text{OH})_2$ ) and quartz ( $\text{SiO}_2$ ) are indicated, while the peaks of corrosion by-products are depicted within the closer view ( $5\text{--}35^\circ$ ) in Figure 13. Furthermore, the peaks of other existing crystalline phases in the coatings, such as olivine, calcite and quartz, are not indicated in Figure 12, although they were included in the quantitative results presented in Figure 14 (i.e., as other phases). It is obvious from the comparison of day zero and day four that the intensity of brucite peaks was reduced over time, due to the reaction of magnesium hydroxide with the sulfuric acid. Apart from the consumption of brucite and periclase, the formation of other by-products, such as magnesium sulfate (hexahydrate,  $\text{MgSO}_4 \cdot 6\text{H}_2\text{O}$ ) and gypsum ( $\text{CaSO}_4 \cdot 2\text{H}_2\text{O}$ ), was also observed (Figure 13). However, the formed magnesium sulfate is rather water-soluble and, thus, it can be easily rinsed from the specimens' surface; therefore, it cannot always be traced after the acid attack. The intensity of gypsum peaks for the coated specimens after spraying is generally smaller than the relevant gypsum peaks of the sprayed uncoated concrete specimen (Figure 12b).

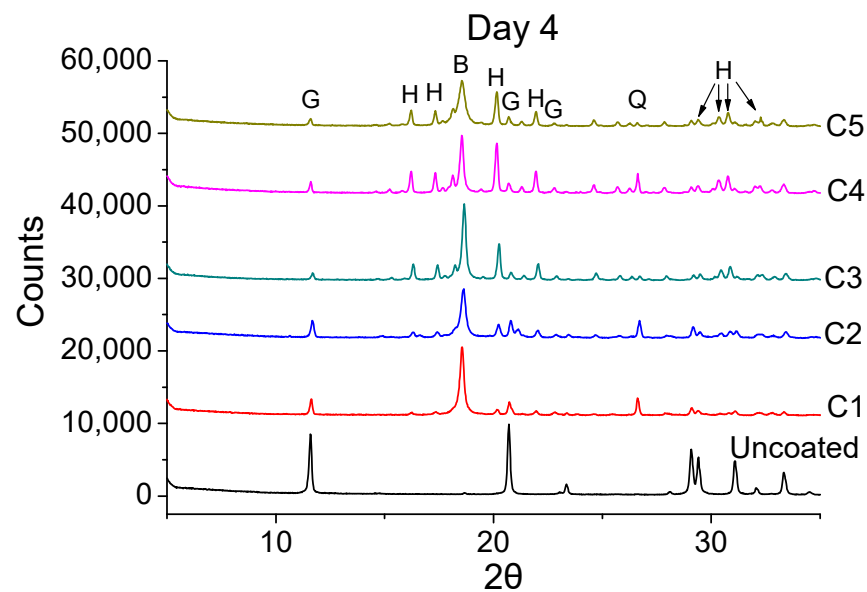


**Figure 13.** XRD overlay diffractograms of Figure 12b depicted between 5–35° of coated and uncoated concrete specimens after four days of the application of the first acid spraying test; G: gypsum, B: brucite, H: hexahydrite, Q: quartz.

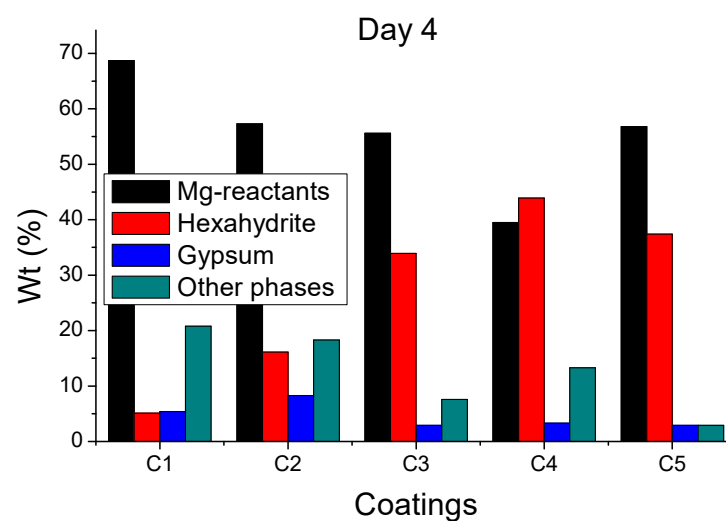


**Figure 14.** The quantitative results of XRD analysis, regarding the presence of crystalline phases for coated concrete specimens after four days of the application of the first acid spraying test.

The gypsum formation may result due to two different reactions: (a) the reaction of sulfuric acid with the small amount of calcium content in the coatings (see Text S2, supplementary material), and (b) the reaction of sulfuric acid with the cement paste of concrete. However, the following results concerning the application of the second acid spraying test (Section 3.4.2) confirm that the initial amount of calcium hydroxide in the coatings (Table 2) was rather small to produce a significant amount of gypsum, as no gypsum was observed to be formed. According to this observation, the formation of gypsum was assumed to result mainly from the reaction of sulfuric acid with the concrete substrate and was used to evaluate the protection properties of coatings against corrosion. In agreement with the results of Figure 12, gypsum was formed in all coated specimens, although in small amounts. Additionally, in the diffractograms of uncoated concrete specimens a lack of hexahydrite peaks is noticed, because of magnesium hydroxide absence. The results of all coating samples after four days of acid spraying, with a concentrated

sulfuric acid solution (4 M) (i.e., following the application of first acid spraying test) were further quantified, by using the Rietveld methodology, and are presented in Figure 14.

The periclase and brucite phases are presented as Mg-reactants, in order to evaluate the overall consumption of magnesium-based components. In the quantitative results of XRD analysis all identified crystalline phases were considered (even those who are not clearly indicated in the diffractograms, i.e., those denoted as other phases). The coating C4 exhibited the largest consumption and the highest production of hexahydrate between all coatings, indicating that the respective coating can be consumed quickly when it reacts with sulfuric acid. This result is in good agreement also with the respective mass change results (Figure 7). The results of coatings C3 and C5 followed that of the previous sample (C4), regarding the noted increase in hexahydrate formation, i.e., increased coating consumption, leading to lower gypsum formation. In contrast, the coating C1 presented the smallest consumption of brucite. As far as the gypsum formation is concerned, the sample of the specimen with coating C2 seemed to present the highest gypsum formation between all examined coatings. This is also in good agreement with the previous results of hardness and roughness changes. It is possible that this specific coating can allow the diffusion of sulfuric acid through its structure and eventually, the acid can reach the concrete surface. In that way the sulfuric acid can react with the cement paste of concrete, resulting to the formation of gypsum and thus negatively affecting the structural properties of concrete. It is obvious that gypsum was identified in all cases but in small amounts, whereas brucite was found in excess quantities; hence, these coatings could keep offering sufficient protection to the concrete substrate.

### 3.4.2. Second Acid Spraying Test

Regarding the XRD results from the second acid spraying test, an overlay of relevant XRD diffractograms, regarding the examined coatings, is shown in Figure 15. The results of coated specimens, sprayed under dry and wet conditions, are depicted in Figure 15a,b, respectively. The intensity of brucite peaks was as high for both dry and wet conditions, as on day zero that as presented in Figure 12a. Additionally, the aforementioned main by-products (i.e., hexahydrate and gypsum) were not identified in this case for both dry- and wet-coating conditions, and after four days of acid spraying. The lower applied concentration of sulfuric acid allowed the coatings to react faster and consume quicker the sprayed acid. In that way, the acid cannot diffuse through the coating and reach the concrete surface, offering a better protection against corrosion. Additionally, the increased number of spraying applications enhanced the rinsing/removal of formed hexahydrate; hence, this crystalline phase cannot be traced.

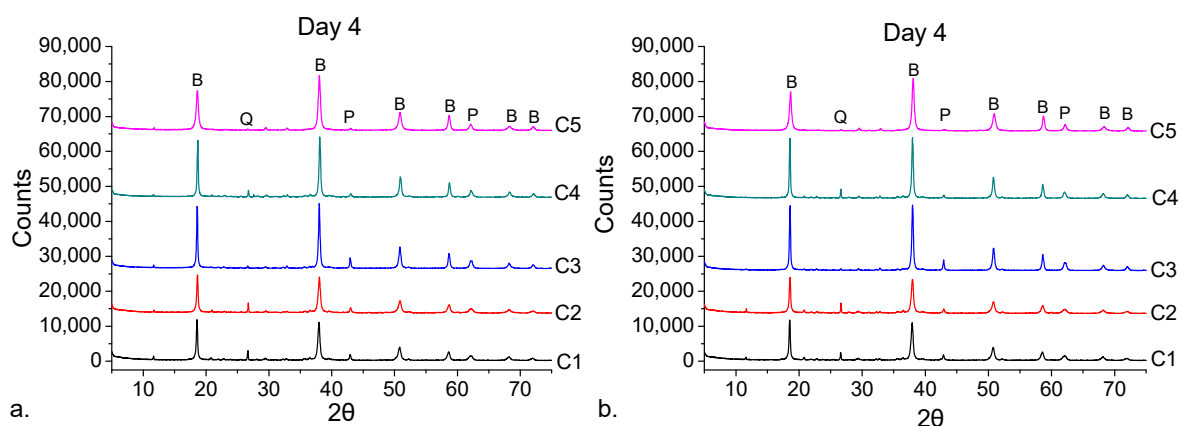


**Figure 15.** XRD overlay diffractograms of coated concrete specimens during (a) dry, and (b) wet coating applications, after four days of the application of the second acid spraying test; P: periclase, B: brucite, Q: quartz.

In order to evaluate better the XRD diffractograms, diffraction patterns were quantified, and the relevant results are presented in Figure 16. For both dry and wet coating conditions, the formed brucite was found in rather large quantities; hence, continued to protect the concrete substrate. On the other hand, the formation of gypsum and hexahydrate was really small (and close to the relevant experimental error), or even zero for the sprayed coated specimens. In practice, there is enough time for the magnesium hydroxide coatings to neutralize the sprayed sulfuric acid (applied in low concentrations) and to offer sufficient anti-corrosion protection to concrete surface. The results of second acid spraying test confirmed also (indirectly) that the formed gypsum during the first acid spraying test was the main reaction product of sulfuric acid with the concrete.

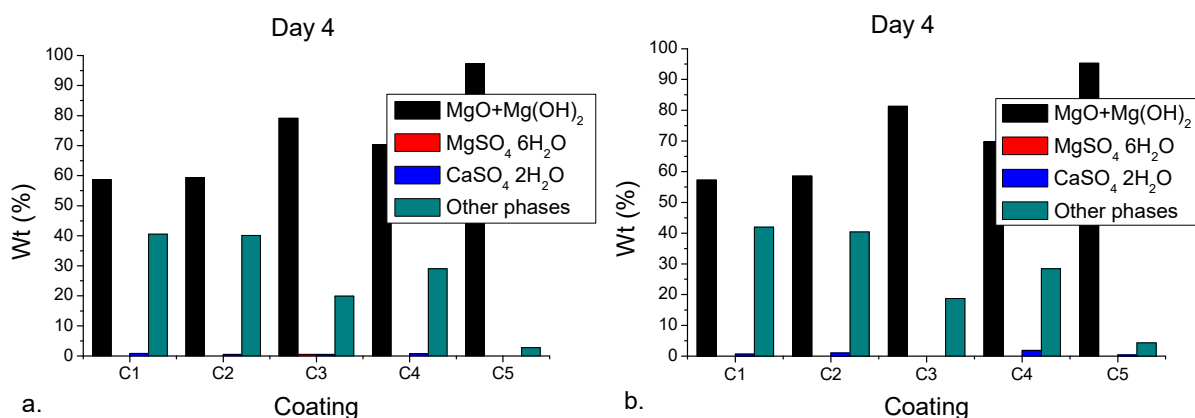


**Figure 16.** The quantitative results of XRD analysis, regarding the crystalline phases of coated concrete specimens during the (a) dry and (b) wet coating applications, after four days of the application of the second acid spraying test.

The existing proportions of the other crystalline phases (i.e., enstatite, olivine) in the C1 and C2 samples were increased, along with the decreased proportions of magnesium reactants, when comparing with the other coatings. According to the chemical composition of MH powders (Table 2), the differences between the powders are rather insignificant. Consequently, the increased proportions of the other phases can be attributed more likely to the decrease of magnesium reactants, because the results are expressed in relative amounts (i.e., as percentages).

#### 4. Discussion

This study aimed to characterize five magnesium hydroxide powders in order to connect their specific physicochemical characteristics with the developed properties of respective coatings. For that reason, the powders mixed with the same proportions of methylcellulose (used as convenient adhesive) and water. The resulting slurries (pastes) were applied onto concrete surface specimens, aiming to protect them against the MIC and the biogenic sulfuric acid in the sewer pipe environment. This procedure was simulated in the laboratory with the application of appropriate accelerated acid spraying tests.

Although the first acid spraying test demonstrated that all examined coatings can be protective against acid corrosion, the application of the second test revealed that the rate of spraying was more important, than the sulfuric acid concentration and can influence the pH evolution of coated specimens. In that way, the coatings C4 and C5 are considered as the most effective ones, when applied under simulated conditions. The protection of sewer pipes against bio-corrosion counts on the application of reactive coatings, which can consume (neutralize) effectively the (biogenic formed) sulfuric acid. Among all the protective coatings, the C4 and the C5 samples are the most suitable ones, relevant with the specific application, as the scope of these coatings is to react with sulfuric acid and to prevent the formation of gypsum, rather to remain simply onto the surface as a protective cover. Noting also that the C5 coating was produced from a high purity raw material and the C4 coating was produced with the addition of a different hydration agent, than the

C1 and C2 coatings. Moreover, the hardness and roughness results of the C4 coating can also indicate the effective protection of the concrete surface, by preserving substantially the concrete surface characteristics.

#### 4.1. Effect of Particle Size Distribution

The particle size distribution of the examined magnesium hydroxide powders was found to influence the behavior of certain coating properties. The larger particles of C1 sample (Table 3) seem to negatively influence the interacting ability of the resulting coating, as the lowest proportion of hexahydrate formation was recorded for this sample. The bigger the size of particles, the slower the interactions with the environment. The particles of the C1 sample were bigger than in the other powders. The slower interacting ability led to the decrease of surface pH at values 6.4 and 6.2 for the dry and wet coatings, respectively (Table 6).

**Table 6.** Summary of magnesium hydroxide powders characteristics and the respective coatings properties; referring (1) to the application of the first acid spraying test, and (2) to the application of the second acid spraying test.

	Mg(OH) <sub>2</sub> Powder				Coated Specimens					
	SSA	PSD <sup>a</sup>	A/B (%) <sup>b</sup>	B (%) <sup>c</sup>	pH1 <sup>d</sup>	pH2 (Dry) <sup>d</sup>	pH2 (Wet) <sup>d</sup>	Hardness2	Thickness1 (%) <sup>e</sup>	Hexahydrate1
C1	low	high	√	x	>8.5	6.4	6.2	-	-26.0	-
C2	low	low	√	x	>8.0	5.2	5.9	x	-30.8	+
C3	low	medium	x	√	>8.0	7.4	8.2	√	-45.1	++
C4	low	medium	√	x	>8.0	8.0	7.9	√	-30.1	+++
C5	high	medium	√	x	>8.0	9.0	8.7	-	-13.6	+++

<sup>a</sup> Particle size distribution of the magnesium hydroxide powder; <sup>b</sup> Adhesion to concrete surface; <sup>c</sup> Cohesion of coating layer; <sup>d</sup> Values at day 4; <sup>e</sup> Variation of the values from day 4 as compared with day 0.

On the other hand, the C3, C4 and C5 coatings/samples, presenting similar particle size distribution and smaller than the sample C1, exhibited better interacting ability even under the application of strong acidic conditions (i.e., when applying the first acid spraying test), as the hexahydrate formation was found in proportions greater than 30%. The latter reflected also to the maintenance of alkaline pH values during all the respective measurements (i.e., pH values > 8.0).

Nevertheless, the adhesion onto the concrete surface seems to be rather independent in relation to the particle size. The coatings C1 and C2, presenting the bigger and the smaller particle size, respectively, showed similar cohesive ability. The smaller particle size of C2 powder reflected only in the density of C2 coating microstructure, as the SEM images revealed. Despite that, the C2 coating was not able to achieve better (alkaline) pH values, than the C3, C4 and C5 coating samples, in order to protect the concrete substrate, as its surface pH values approached 5.2 during the dry coating application test.

#### 4.2. Effect of Specific Surface Area and Purity

The SSA hardly influenced the properties of prepared coatings. The sample C4 with the smaller SSA presented similar results to the sample C5 having the highest SSA value. The hexahydrate formation was found to be increased and the gypsum formation to be decreased in both coatings during the first acid spraying test application. The pH stability during the spraying test of dry and wet coatings showed that magnesium hydroxides with SSAs between 10–32 m<sup>2</sup>/g can offer a sufficient alkaline (protective) surface.

Additionally, the type of adhesion failure onto the concrete surface was not affected by the variations of SSA, as the failure type between coatings with different SSAs (i.e., C4 and C5 samples) did not substantially differ (Table 4). However, the coatings' tensile bond strength seemed to be influenced by the coatings' SSA. The C5 sample with the largest SSA value, presented the smallest value of tensile bond strength, while the C3 sample with the

smallest SSA value, presented the largest value of tensile bond strength. The rest of the coatings presented intermediate SSA and bond strength values.

The increased (alkaline) values of surface pH for sample C5, in both acid spraying tests, may result from this coating's higher SSA value, along with the aforementioned influence of the particle size.

Another factor that can contribute to the resulting properties of coatings was the purity of raw materials (CCM) that were used to produce the MH powders, which were used for the preparation of the coatings. The MgO content (%wt.) of the raw materials used for the samples C3 and C5 was found to be 90.3% and 91.77%, respectively. The resulting coatings from these materials were found to be able to preserve the surface pH values always above pH 8 (pH<sub>2</sub> wet, Table 6). On the other hand, the raw materials, used for the preparation of samples C1 and C2, contained around 82% MgO. The resulting coatings presented pH values lower than 6.4. As a result, it seems that the purity of raw materials also plays an important role on the behavior of the produced coatings. Indeed, the increased purity allows the preservation of sufficient alkaline pH values when the applied coating is tested under wet hydration conditions.

## 5. Conclusions

The main physicochemical characteristics of magnesium hydroxide powders may affect the properties of the produced coatings, regarding the protection of concrete structure against (biogenic) sulfuric acid attack. The results of this research showed that the particle size distribution of powders, used for the preparation of coatings, can influence the interacting ability of the coating with the acid. Additionally, it was demonstrated that the specific surface area of Mg(OH)<sub>2</sub> powders does not affect the anti-corrosion performance of the applied coating. The frequent spraying rate proved to be more important than the sulfuric acid concentration for the efficient pH maintenance of concrete surface in the desired alkaline values.

All magnesium hydroxide coatings seemed to offer sufficient protection against acid attack, provoking the corrosion of concrete substrates, but in different degrees, depending on the specific characteristics and properties of the raw materials used. However, it is important to select raw materials with appropriate properties, such as the well-distributed particle size, and the high purity of raw caustic calcined magnesia, in order to be able to achieve the optimal corrosion protection of concrete surfaces.

**Supplementary Materials:** The following are available online at <https://www.mdpi.com/article/10.3390/w13091227/s1>, Text S1: Concrete specimens, Text S2: Stoichiometry calculations, Table S1: Quantitative results regarding the main mineralogical phases of the five magnesium hydroxide powders (%). Figure S1: Maximum pH values obtained after 1 min of the addition of each drop of the sulfuric acid solution in the MH solutions. The maximum pH values obtained after 1 min of the addition of 1 drop (~0.5 mL) of sulfuric acid solution, in a dispersion of each magnesium hydroxide powder (0.5 g MH/100 mL of deionized water). The acid was added at the rate of one drop/min, Figure S2: Steps of pull-off measurements; (a) coating applied onto the cyclical concrete surface, (b) dollies stuck onto the coating surface, and (c) dollies with coating and adhesive after the pull-off measurement, Figure S3: Type of pull-off failures (a) 100% A/B type of failure, (b) 100% B type of failure, Figure S4: SEM-micrographs of the coated concrete specimens with the coatings; (a) C1, (b) C3 and (c) C5. The coatings are presented in the upper side, whereas the concrete is presented in the lower side of each image.

**Author Contributions:** Conceptualization, E.K.A., H.Y. and A.Z.; methodology, D.M. and E.-C.T.; validation, D.M. and E.-C.T.; investigation, D.M. and E.-C.T.; resources, E.K.A., H.Y. and A.Z.; data curation, D.M. and E.-C.T.; writing—original draft preparation, D.M. and E.-C.T.; writing—review and editing, E.K.A., H.Y. and A.Z.; supervision, E.K.A., H.Y. and A.Z.; project administration, E.K.A., H.Y. and A.Z. All authors have read and agreed to the published version of the manuscript.

**Funding:** This research has been co-financed by the European Union and Greek national funds through the Operational Program Competitiveness, Entrepreneurship and Innovation, under the call RESEARCH-CREATE-INNOVATE (project code: T1EDK-02355).

**Institutional Review Board Statement:** Not applicable.

**Informed Consent Statement:** Not applicable.

**Data Availability Statement:** The data presented in this study are available upon request from the corresponding author.

**Acknowledgments:** This research has been co-financed by the European Union and Greek national funds through the Operational Program Competitiveness, Entrepreneurship and Innovation, under the call RESEARCH–CREATE–INNOVATE (project code: T1EDK-02355).

**Conflicts of Interest:** The authors declare no conflict of interest.

## References

1. Roghanian, N.; Banthia, N. Development of a sustainable coating and repair material to prevent bio-corrosion in concrete sewer and waste-water pipes. *Cem. Concr. Compos.* **2019**, *100*, 99–107. [[CrossRef](#)]
2. Aguiar, J.B.; Camões, A.; Moreira, P.M. Coatings for Concrete Protection against Aggressive Environments. *J. Adv. Concr. Technol.* **2008**, *6*, 243–250. [[CrossRef](#)]
3. Berndt, M. Evaluation of coatings, mortars and mix design for protection of concrete against sulphur oxidising bacteria. *Constr. Build. Mater.* **2011**, *25*, 3893–3902. [[CrossRef](#)]
4. ASCE (American Society of Civil Engineers); WPCF (Water Pollution Control Federation). *Gravity Sanitary Sewer Design and Construction*; American Society of Civil Engineers: Reston, VA, USA, 2007. [[CrossRef](#)]
5. Parker, C. The corrosion of concrete. The isolation of a species of bacterium associated with the corrosion of concrete exposed to atmospheres containing hydrogen sulfide. *Aust. J. Exp. Biol. Med. Sci.* **1945**, *23*, 81–90. [[CrossRef](#)]
6. Parker, C. The corrosion of concrete. The function of Thiobacillus Concretivorus in the corrosion of concrete exposed to atmospheres containing hydrogen sulfide. *Aust. J. Exp. Biol. Med. Sci.* **1945**, *23*, 91–98. [[CrossRef](#)]
7. Parker, C.D. Species of Sulphur Bacteria Associated with the Corrosion of Concrete. *Nature* **1947**, *159*, 439–440. [[CrossRef](#)] [[PubMed](#)]
8. Islander, R.L.; Deviny, J.S.; Mansfeld, F.; Postyn, A.; Shih, H. Microbial Ecology of Crown Corrosion in Sewers. *J. Environ. Eng.* **1991**, *117*, 751–770. [[CrossRef](#)]
9. Wu, M.; Wang, T.; Wu, K.; Kan, L. Microbiologically induced corrosion of concrete in sewer structures: A review of the mechanisms and phenomena. *Constr. Build. Mater.* **2020**, *239*, 117813. [[CrossRef](#)]
10. Hvitved-Jacobsen, T.; Vollertsen, J.; Nielsen, A.H. *Sewer Processes: Microbial and Chemical Process Engineering of Sewer Networks*; CRC Press: Cleveland, OH, USA, 2013.
11. Okabe, S.; Odagiri, M.; Ito, T.; Satoh, H. Succession of Sulfur-Oxidizing Bacteria in the Microbial Community on Corroding Concrete in Sewer Systems. *Appl. Environ. Microbiol.* **2007**, *73*, 971–980. [[CrossRef](#)] [[PubMed](#)]
12. Mori, T.; Nonaka, T.; Tazaki, K.; Koga, M.; Hikosaka, Y.; Noda, S. Interactions of nutrients, moisture and pH on microbial corrosion of concrete sewer pipes. *Water Res.* **1992**, *26*, 29–37. [[CrossRef](#)]
13. Wells, T.; Melchers, R.E. *Findings of a 4 Year Study of Concrete Sewer Pipe Corrosion*; Australasian Corrosion Association: Preston, VIC, Australia, 2014.
14. Wells, T.; Melchers, R.E.; Bond, P. *Factors Involved in the Long Term Corrosion of Concrete Sewers*; Semantic Scholar: Seattle, WA, USA, 2009.
15. Sydney, R.; Esfandi, E.; Surapaneni, S. Control Concrete Sewer Corrosion via the Crown Spray Process. *Water Environ. Res.* **1996**, *68*, 338–347. [[CrossRef](#)]
16. Wang, T.; Wu, K.; Kan, L.; Wu, M. Current understanding on microbiologically induced corrosion of concrete in sewer structures: A review of the evaluation methods and mitigation measures. *Constr. Build. Mater.* **2020**, *247*, 118539. [[CrossRef](#)]
17. Araghi, H.J.; Nikbin, I.; Reskati, S.R.; Rahmani, E.; Allahyari, H. An experimental investigation on the erosion resistance of concrete containing various PET particles percentages against sulfuric acid attack. *Constr. Build. Mater.* **2015**, *77*, 461–471. [[CrossRef](#)]
18. Vincke, E.; Van Wanseele, E.; Monteny, J.; Beeldens, A.; De Belie, N.; Taerwe, L.; Van Gemert, D.; Verstraete, W. Influence of polymer addition on biogenic sulfuric acid attack of concrete. *Int. Biodeterior. Biodegrad.* **2002**, *49*, 283–292. [[CrossRef](#)]
19. Nielsen, A.H.; Vollertsen, J.; Jensen, H.S.; Wium-Andersen, T.; Hvitved-Jacobsen, T. Influence of pipe material and surfaces on sulfide related odor and corrosion in sewers. *Water Res.* **2008**, *42*, 4206–4214. [[CrossRef](#)] [[PubMed](#)]
20. James, J. Controlling sewer crown corrosion using the crown spray process with magnesium hydroxide. *Proc. Water Environ. Fed.* **2003**, *2003*, 259–268. [[CrossRef](#)]
21. Merachtsaki, D.; Fytianos, G.; Papastergiadis, E.; Samaras, P.; Yiannoulakis, H.; Zouboulis, A. Properties and Performance of Novel Mg(OH)<sub>2</sub>-Based Coatings for Corrosion Mitigation in Concrete Sewer Pipes. *Materials* **2020**, *13*, 5291. [[CrossRef](#)] [[PubMed](#)]
22. Monteny, J.; De Belie, N.; Vincke, E.; Verstraete, W.; Taerwe, L. Chemical and microbiological tests to simulate sulfuric acid corrosion of polymer-modified concrete. *Cem. Concr. Res.* **2001**, *31*, 1359–1365. [[CrossRef](#)]
23. Wells, T.; Melchers, R. An observation-based model for corrosion of concrete sewers under aggressive conditions. *Cem. Concr. Res.* **2014**, *61–62*, 1–10. [[CrossRef](#)]

24. Diamanti, M.V.; Brenna, A.; Bolzoni, F.; Berra, M.; Pastore, T.; Ormellese, M. Effect of polymer modified cementitious coatings on water and chloride permeability in concrete. *Constr. Build. Mater.* **2013**, *49*, 720–728. [[CrossRef](#)]
25. European Committee for Standardization. *EN 1542:1999: Products and Systems for the Protection and Repair of Concrete Structures—Test Methods—Measurement of Bond Strength by Pull-Off*; BSI: London, UK, 1999.
26. European Committee for Standardization. *EN 13578:2003: Products and Systems for the Protection and Repair of Concrete Structures—Test Methods—Compatibility on Wet Concrete*; BSI: London, UK, 2003.